EPJ Web of Conferences **49**, 12001 (2013)
DOI: 10.1051/epjconf/20134912001

A new implementation of the NMSSM Higgs boson decays

J. Baglio[1,a], T. N. Dao[1], R. Gröber[1], M. M. Mühlleitner[1], H. Rzehak[2,3], M. Spira[4], J. Streicher[1], and K. Walz[1]

[1] *Institut für Theoretische Physik, KIT, Germany*
[2] *Theory Group, CERN, Switzerland*
[3] *Physikalisches Institut, Universität Freiburg, Germany*
[4] *Theory Department, Paul Scherrer Institute, Switzerland*

Abstract. Supersymmetric theories provide elegant extensions of the Standard Model. Among these the NMSSM is a model which in addition to the content of the MSSM includes a new singlet to solve the μ problem. We present here the basic features of the NMSSM Higgs sector and a new Fortran implementation of the decays of the Higgs bosons in the NMSSM, both with real and complex parameters.

1 Introduction

Now that a new boson has been discovered by the ATLAS and CMS Collaborations [1, 2], an important question remains to be solved: is it the Standard Model (SM) Higgs boson or some exotic beyond the SM (BSM) Higgs particle? Among the various BSM models, supersymmetric (SUSY) extensions are the primary candidates to solve various problems of the SM, as for example the hierarchy problem. The Next–to–Minimal Supersymmetric SM (NMSSM) is a SUSY extension where in addition to two Higgs doublets H_u and H_d a Higgs singlet field S is included to dynamically generate the μ–term, thereby solving the so-called " μ–problem" of the MSSM. Indeed, a SUSY invariant term $\mu H_u \cdot H_d$ can be found in the MSSM Lagrangian. The coupling μ, being a parameter with mass dimension not linked to any SUSY–breaking scale, is naturally of the order of the largest scale available in the theory (or equal to zero), see Ref. [3]. This is in contradiction to phenomenological requirements that μ is of the order of the electroweak scale, unless a high level of fine–tuning is involved. By dynamically generating the μ–term in the NMSSM through the singlet Higgs vacuum expectation value v_s in the trilinear coupling $\lambda S H_u \cdot H_d$, $\mu^{\rm eff} = \lambda v_s/\sqrt{2}$, this fine–tuning problem is avoided. The Higgs sector is then less restricted: the tree-level bound on the lightest Higgs boson mass is higher than in the MSSM, meaning that smaller quantum corrections are required to get $M_h \sim 126$ GeV for the SM–like Higgs boson. A review of the NMSSM can be found in Ref. [4, 5].

Using complex parameters gives rise to CP violation in the model as required by the baryon asymmetry in the Universe, by its implementation already at tree–level in the NMSSM Higgs sector for example. In addition, the phenomenology of the Higgs bosons is substantially modified as all the Higgs states can mix and there are no pure CP–even or CP–odd states anymore. In order to compare with recent experimental results it is mandatory to assess, besides the spectrum, the decay pattern of the NMSSM Higgs bosons. In the following, we will present our implementation of the NMSSM Higgs boson decays either with real (CP–conserving $\mathbb{R}$–NMSSM) or complex (CP–violating $\mathbb{C}$–NMSSM) parameters. In particular the state-of-the-art higher–order corrections will be included as well as the renormalization group evolution of the parameters.

2 The NMSSM Higgs sector

2.1 Parametrization

In this section we concentrate on the (complex) Higgs sector and its parametrization. The NMSSM superpotential gives rise to the following scalar Higgs potential,

$$\begin{aligned} V =& |\lambda|^2|S|^2\left(H_u^\dagger H_u + H_d^\dagger H_d\right) + \left|\lambda\left(H_u^\intercal \epsilon H_d\right) + \kappa S^2\right|^2 + \\ & \frac{1}{2}g_2^2|H_u^\dagger H_d|^2 + \frac{1}{8}(g_1^2+g_2^2)\left(H_u^\dagger H_u - H_d^\dagger H_d\right)^2 + \\ & m_{H_u}^2 H_u^\dagger H_u + m_{H_d}^2 H_d^\dagger H_d + m_S^2|S|^2 + \\ & \left(\lambda A_\lambda\left(H_u^\intercal \epsilon H_d\right) S + \frac{1}{3}\kappa A_\kappa S^3 + \text{c.c}\right), \end{aligned} \tag{1}$$

with complex λ, κ, A_λ and A_κ. We then introduce the vacuum expectation values for the Higgs fields and use the following parametrization with the phases ϕ_u, ϕ_s,

$$\begin{aligned} H_d &= \frac{1}{\sqrt{2}}\begin{pmatrix} v_d + h_d + i\,a_d \\ \sqrt{2}\,H_d^- \end{pmatrix}, \quad H_u = \frac{e^{i\,\phi_u}}{\sqrt{2}}\begin{pmatrix} \sqrt{2}\,H_u^+ \\ v_u + h_u + i\,a_u \end{pmatrix} \\ S &= \frac{e^{i\,\phi_s}}{\sqrt{2}}\left(v_s + h_s + i\,a_s\right). \end{aligned} \tag{2}$$

[a] Speaker; e-mail: baglio@particle.uni-karlsruhe.de

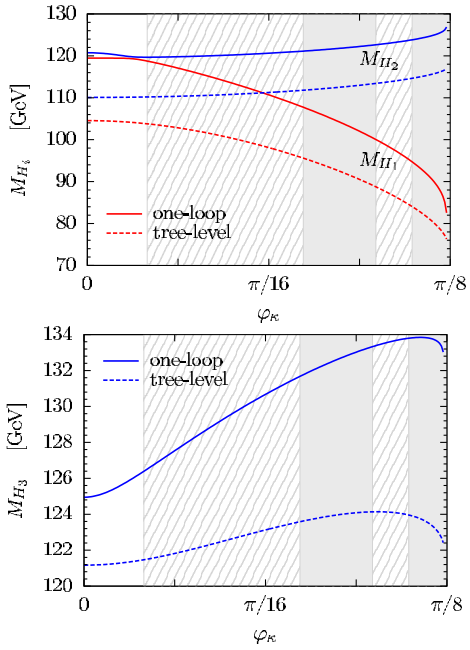

Figure 1. Upper panel: tree–level (dashed) and one–loop masses (full) for H_1 and H_2 states for a $\mathbb{C}$–NMSSM scenario. Lower panel: same for the H_3 state. The exclusion region due to LEP, Tevatron and 7 TeV LHC data is shown as a grey area, the region with the SM-like Higgs boson not being compatible with an excess of data around 125 GeV as dashed area. The figures have been taken from Ref. [7].

In the Higgs sector there are only six CP–violating phases that are needed in the scalar potential: ϕ_u, ϕ_s, ϕ_λ, ϕ_κ, ϕ_{A_λ} and ϕ_{A_κ}. In other sectors of the model further CP–violating phases appear such as those of M_1, M_2, etc. Among the six phases described above, only one single combination is actually relevant at tree–level,

$$\Psi = \phi_\lambda - \phi_\kappa + \phi_u - 2\phi_s\,, \tag{3}$$

the other possible combinations being fixed by tadpole conditions [4, 5].

2.2 Higgs boson masses at one–loop level

Higher order corrections to the masses of the Higgs bosons are available at one–loop in the $\mathbb{R}$–NMSSM [6] and in the $\mathbb{C}$–NMSSM [7], and even up to two–loop order in the $\mathbb{R}$–NMSSM [8]. In Refs. [6, 7] a mixed renormalization scheme was used in which on–shell renormalization was used for the physical parameters while the $\overline{\rm DR}$ scheme was used to renormalize the parameters $\tan\beta$, v_s, $|\lambda|$, $|\kappa|$, $|A_\kappa|$ and the phases in case of the $\mathbb{C}$–NMSSM. It has been shown that all the counter-terms for the phases, with the exception of the phases linked to the two tadpole conditions t_a and t_{a_s}, vanish [7].

The effects of quantum corrections are sizeable. We display two cases taken from Ref. [7], first with tree–level CP violation where $\Psi \neq 0$, more precisely $\phi_\kappa \neq 0$, $\phi_\lambda = \phi_u = \phi_s = 0$, then without tree–level CP violation where $\Psi = 0$ but with $\phi_\lambda = \phi_\kappa$ and $\phi_\kappa \neq 0$.

One–loop corrections to the masses are of utmost importance to conduct realistic studies, as can be seen in

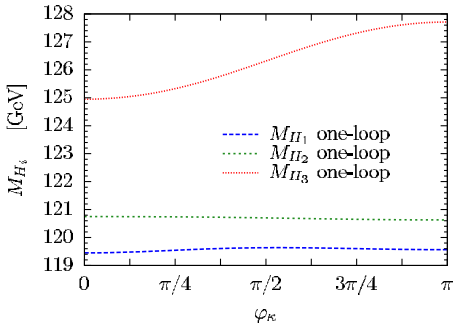

Figure 2. The one–loop masses for the H_1, H_2 and H_3 states for a $\mathbb{C}$–NMSSM scenario without tree–level CP violation. The figure has been taken from Ref. [7].

Fig. 1 where the tree–level (one–loop) masses are depicted with dashed (full) lines, and the H_3 state plays the role of the SM–like Higgs boson. Only with one–loop masses the scenario becomes consistent with the Higgs search results of $M_{H_{\rm SM}} \simeq 125$ GeV. The dashed area shows the region not compatible with this requirement at one–loop, the grey area shows the region not compatible with exclusion limits from the LEP, Tevatron and 7 TeV LHC data. In the case with no CP violation at tree–level but still non vanishing phases ϕ_λ, ϕ_κ, the impact of the latter is negligible for the H_1 and H_2 states. The stronger the coupling to the stops is, the stronger the one–loop corrections to the Higgs boson mass are influenced, the stop mass being a ffected by ϕ_λ. As in this scenario $\phi_\lambda = \phi_\kappa$, the heavier H_3 mass increases with increasing $\phi_\kappa (= \phi_\lambda)$ as can be seen in Fig. 2 while the H_1 and H_2 masses remain nearly constant, H_3 having a large h_u component strongly coupled to the stops. Note also that again the quantum corrections are not negligible as they increase M_{H_3} by 3 – 6% as shown in Ref. [7].

3 The Higgs boson decays

3.1 Description of the Fortran implementation

Our new implementation of the decays of the NMSSM Higgs bosons uses the one–loop masses decribed in section 2.2 as input masses. We have built a Fortran code for the decays of the NMSSM Higgs bosons based on the program `HDECAY` [9, 10]. The user can choose to use either real (CP–conserving) or complex (CP–violating) parameters with CP–violating phases in the Higgs sector. Higher order corrections are included in the relevant decays as well as the renormalization group equations (RGEs) at one loop in the $\mathbb{R}$–NMSSM [11, 12]. The implementation of the RGEs in the $\mathbb{C}$–NMSSM is still work in progress.

3.2 Comparison between the $\mathbb{R}$–NMSSM and the $\mathbb{C}$–NMSSM

In order to show the potential of the code, we have started preliminary analyses. We start from real NMSSM benchmark points [12] and tune the phases with two requirements:

- the SM–like Higgs state should reproduce the observed excess within a 10 GeV range, 120 GeV $\leq M_{H_{\rm SM}} \leq$ 130 GeV;

Table 1. The set of parameters used in the study of section 3.

$\|\lambda\| = 0.71$	$\|\kappa\| = 0.34$	$\tan\beta = 2$	$v_s = 354.5$ GeV	$Q = 540$ GeV
$\|A_\kappa\| = 35.5$ GeV	$\|A_b\| = 1$ TeV	$A_t = 1.5$ TeV	$A_\ell = 1$ TeV	$M_{\rm SUSY} = 2.5$ TeV
$M_1 = 130$ GeV	$M_2 = 260$ GeV	$M_3 = 1$ TeV	$M_{\tau_R} = M_{L_3} = 300$ GeV	$M_{t_R} = M_{Q_3} = 540$ GeV

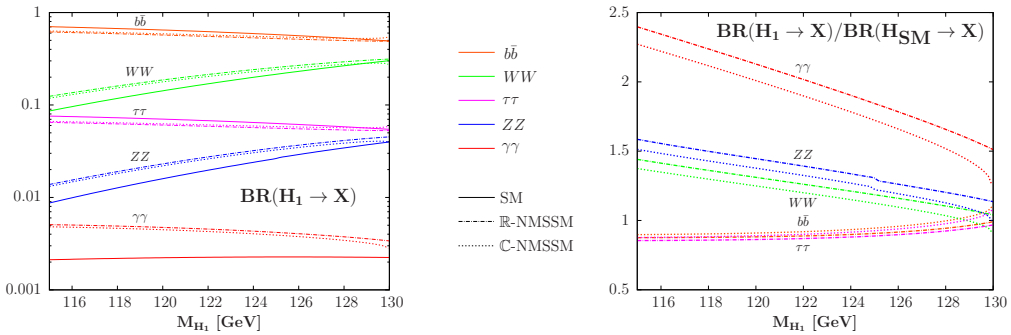

Figure 3. Left: the decay branching fractions of the lightest Higgs state H_1 into $b\bar{b}$ (orange line), WW^* (green line), $\tau^+\tau^-$ (violet line) ZZ^* (blue line) and $\gamma\gamma$ (red line) as a function of the Higgs mass M_{H_1} (in GeV). The full lines are the SM predictions, the dashed-dotted lines are the $\mathbb{R}$–NMSSM predictions and the dotted lines are the $\mathbb{C}$–NMSSM predictions. Right: the same but for the ratio between the NMSSM and the SM branching fractions.

- the phases ϕ_{A_λ} and ϕ_{A_κ} are fixed by tadpole conditions, $\phi_\lambda = \phi_\kappa = \phi_s = 0$ and $\phi_u \neq 0$. We start with a fixed value $\phi_u = 0.1$.

The set of parameters is given in Table 1. All the parameters are set at the SUSY scale $Q = 540$ GeV in the $\overline{\rm DR}$ scheme.

We display in Fig. 3 the decay branching fractions for the H_1 state as a function of the Higgs mass M_{H_1} obtained when varying $|A_\lambda|$. On the left–hand side the branching ratios are depicted, on the right–hand side the ratio between the branching ratios and the SM predictions is displayed. We show a comparison between the SM, the $\mathbb{C}$–NMSSM and the $\mathbb{R}$–NMSSM. In the latter model we use the same set of parameters described above but with the phases turned to zero. The NMSSM branching fractions are higher than those of the SM except for $H_1 \to b\bar{b}$ and $H_1 \to \tau^+\tau^-$ so that the sum of the branching fractions is equal to 1. The shapes are similar in the real and complex NMSSM as shown in Fig. 3, with the notable exception in the region near $M_{H_1} = 130$ GeV, where the $\mathbb{C}$–NMSSM predictions are much closer to the SM predictions than in the real NMSSM case.

We display in Figs. 4 and 5 the branching fractions in two specific channels to comment in more detail on the decay pattern. Starting with the decay $H_1 \to b\bar{b}$, Fig. 4 shows that the NMSSM predictions are smaller than the SM predictions. Nevertheless, the $\mathbb{C}$–NMSSM branching fraction is always closer to the SM prediction than the $\mathbb{R}$–NMSSM prediction. There is even a cross–over at $M_{H_1} \simeq 128$ GeV (the same cross–over is found in the $H \to WW^*$ branching fraction) where the $\mathbb{C}$–NMSSM prediction matches the SM branching fraction. The same comment can also be made for the decay $H_1 \to \tau^+\tau^-$.

It can be noted that in this particular case turning on the phases in the Higgs sector helps to reproduce the observed value of the signal strength in the diphoton channel $\sigma^{\rm obs}/\sigma^{\rm SM} \simeq 1.8$ at $M_H = 125$ GeV as can be seen in

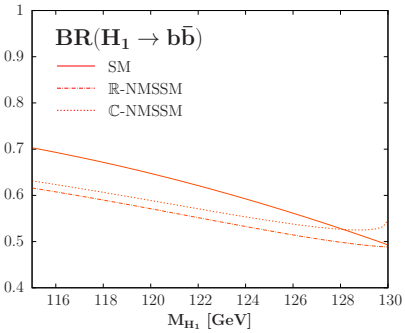

Figure 4. The decay branching fraction of the lightest Higgs state H_1 into $b\bar{b}$ as a function of the Higgs mass M_{H_1} (in GeV). The full line is the SM prediction, the dashed-dotted line is the $\mathbb{R}$–NMSSM prediction and the dotted line is the $\mathbb{C}$–NMSSM prediction.

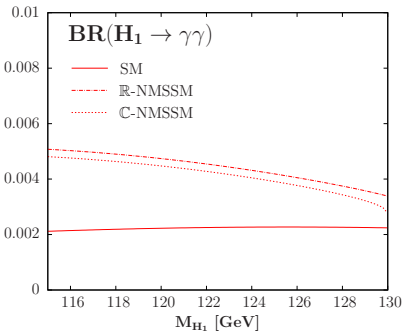

Figure 5. The decay branching fraction of the lightest Higgs state H_1 into $\to \gamma\gamma$ as a function of the Higgs mass M_{H_1} (in GeV). The full line is the SM prediction, the dashed-dotted line is the $\mathbb{R}$–NMSSM prediction and the dotted line is the $\mathbb{C}$–NMSSM prediction.

Fig. 5. In this decay the situation is inverted compared to $H \to b\bar{b}$ decay and the SM prediction is the lowest. This is due to the reduced decay width into $b\bar{b}$, which is the dominant decay, hence it induces a smaller total decay width

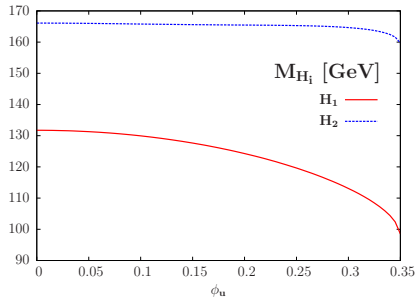

Figure 6. H_1 and H_2 masses (in GeV) in the $\mathbb{C}$–NMSSM scenario described in the text as a function of the phase ϕ_u.

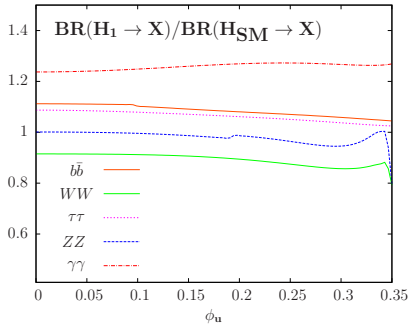

Figure 7. The ratio between H_1 decay branching fractions in the $\mathbb{C}$–NMSSM and the SM predictions for the same mass as a function of the phase ϕ_u.

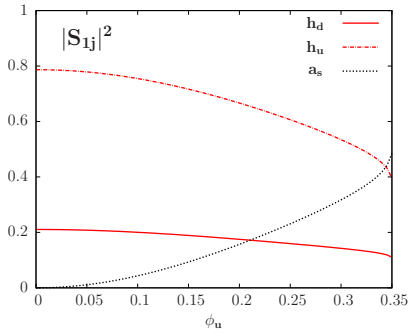

Figure 8. The decomposition of the lightest Higgs state H_1 in terms of the Higgs electroweak eigenstates as a function of the phase ϕ_u.

and therefore an enhanced diphoton branching ratio. This means that although reducing the deviations from the SM, the $\mathbb{C}$–NMSSM scenario can nevertheless account for the excess of the data in the diphoton channel[1].

3.3 Phase variation in the $\mathbb{C}$–NMSSM

We now modifiy the set-up of section 3.2. The phase ϕ_u is not fixed anymore and varies in the range $0 \leq \phi_u \leq 0.35$, starting from an $\mathbb{R}$–NMSSM scenario ($\phi_u = 0$). Above the upper limit of $\phi_u = 0.35$ the tadpole conditions cannot be fulfilled and the model is not valid anymore. The goal is to demonstrate the sensitivity of the Higgs boson decays to the complex phases in the Higgs sector. In our particular example the variation of the phase ϕ_u has a significant impact on the branching fractions. Note that the chosen scenario for this particular example is not required to fulfill collider constraints when the phase ϕ_u is different from $\phi_u = 0.1$.

We display in Fig. 6 the masses of the two lightest Higgs states H_1 and H_2 as a function of the phase ϕ_u. The lightest mass is strongly affected by the variation of ϕ_u and $M_{H_1} \simeq 125$ GeV is obtained for $\phi_u = 0.2$. The heavier state H_2, however, has a nearly constant mass all over the range, $M_{H_2} \simeq 167$ GeV. Interestingly enough, while the mass of the state H_1 is strongly affected by the phase ϕ_u, the branching fractions are hardly modified when increasing ϕ_u (except for $\phi_u \geq 0.30$), as depicted in Fig. 7. The decomposition of the lightest Higgs state H_1 in terms of the electroweak eigenstates is shown in Fig. 8, where $|S_{1j}|^2$ is the square of the absolute value of the mixing term between H_1 and the electroweak eigenstate Φ_j: $H_i = \sum_{i=1\ldots5} S_{ij}\Phi_j$, $\Phi = (h_d, h_u, h_s, a, a_s)^T$. Three distinct regions can be identified,

- $\phi_u \leq 0.1$: the lightest H_1 state is nearly a pure CP–even doublet state, close to what would be expected for a SM–like Higgs boson;
- $0.1 < \phi_u \leq 0.2$: H_1 is still mostly a CP–even doublet state but the singlet a_s component increases;
- $\phi_u > 0.2$: H_1 is a CP–mixed state with singlet admixture, the a_s component being more important than the h_d component.

[1]This assumes that the production cross sections are not strongly affected by the phases. This has to be confirmed, though.

Even though H_1 is a specific $\mathbb{C}$–NMSSM state and even though its mass is strongly affected by the phase ϕ_u, its decay branching fractions are hardly affected in this scenario.

The case of the heavier state H_2 is very different. The decomposition into electroweak eigenstates again shows three distinct regions, see Fig. 9:

- $\phi_u \leq 0.03$: the H_2 state is a pure singlet state nearly CP–even;
- $0.03 < \phi_u \leq 0.27$: H_2 is still mostly a singlet state but there is a strong CP mixing between the h_s and a_s states. There is a cross–over at $\phi \simeq 0.27$ where a_s becomes the dominant singlet component;
- $\phi_u > 0.27$: H_2 is a CP–mixed state with a strong mixing between the singlet and the doublet components. There is a cross–over at $\phi \simeq 0.33$ where the CP–even h_d state dominates over the CP–odd h_s state.

Nevertheless, although M_{H_2} is nearly constant when varying ϕ_u, the decay pattern is strongly affected by the variation of the phase ϕ_u. Indeed, as can be seen in Fig. 10 (upper), the branching fractions of the decays $H_2 \to b\bar{b}, \tau^+\tau^-$ are strongly enhanced, by up to a factor of $75 - 85$ at $\phi_u \simeq 0.065$. A zoom on the smaller decay branching fractions in Fig. 10 (lower) shows that this strong enhancement at $\phi_u \simeq 0.065$ corresponds to a suppression of the decays into weak bosons. The decay $H_2 \to \gamma\gamma$ is also enhanced with a branching fraction five times higher than in the SM.

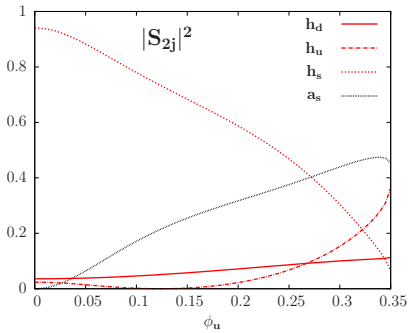

Figure 9. The decomposition of the heavier Higgs state H_2 in terms of the Higgs electroweak eigenstates as a function of the phase ϕ_u

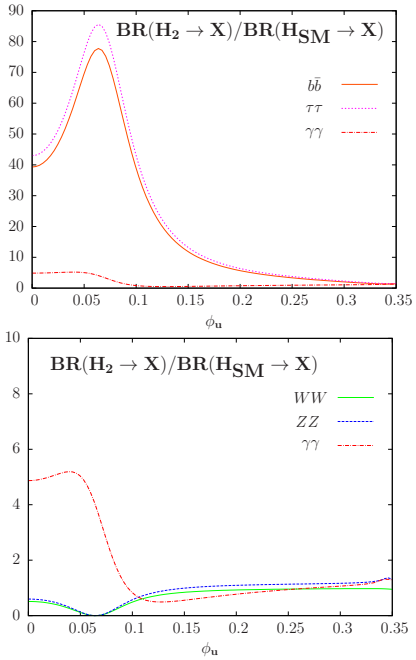

Figure 10. Upper panel: the ratio between the H_2 branching fractions in the ℂ–NMSSM and the SM predictions for the same mass as a function of the phase ϕ_u. Lower panel: the same but with a zoom on the small branching fractions.

4 Conclusion

We have presented the characteristic features of the Higgs sector in the NMSSM using complex parameters in order to take into account *CP*-violating effects in the Higgs sector already at tree-level. We have implemented the decays of the NMSSM Higgs bosons within the real and the complex NMSSM in a Fortran code based on `HDECAY`. The implementation includes the available higher–order corrections as well as the renormalization group evolutions, in the ℝ–NMSSM, of the input parameters at one–loop order. As shown in section 2.2, it is necessary to use the input Higgs masses at higher order which has been done in our implementation. Preliminary results have been discussed in section 3 and show that in some cases the deviation in the branching fractions with respect to the SM can be reduced when turning the complex phases on. The decay pattern can also be strongly affected by the complex phases with a large increase in some decay channels. A public version of the code will soon be available [13]. Updates of the code, as e.g. the implementation of the RGEs in the case of the ℂ–NMSSM, will follow.

Acknowledgements

J.B. would like to thank the organizers for the nice atmosphere during the conference as well as for the possibility to give a talk. This work is supported by the Deutsche Forschungsgemeinschaft via the Sonderforschungsbereich/Transregio SFB/TR-9 Computational Particle Physics.

References

[1] G. Aad et al. (ATLAS Collaboration), Phys.Lett. **B716**, 1 (2012).
[2] S. Chatrchyan et al. (CMS Collaboration), Phys.Lett. **B716**, 30 (2012).
[3] D. Miller, R. Nevzorov, P. Zerwas, Nucl.Phys. **B681**, 3 (2004).
[4] M. Maniatis, Int.J.Mod.Phys. **A25**, 3505 (2010).
[5] U. Ellwanger, C. Hugonie, A. Teixeira, Phys.Rept. **496**, 1 (2010).
[6] K. Ender, T. Graf, M. Mühlleitner, H. Rzehak, Phys.Rev. **D85**, 075024 (2012) and references therein.
[7] T. Graf, R. Gröber, M. Mühlleitner, H. Rzehak, K. Walz, JHEP **10**, 122 (2012) and references therein.
[8] G. Degrassi, P. Slavich, Nucl.Phys. **B825**, 119 (2010).
[9] A. Djouadi, J. Kalinowski, M. Spira, Comput.Phys.Commun. **108**, 56 (1998).
[10] A. Djouadi, M. Mühlleitner, M. Spira, Acta Phys.Polon. **B38**, 635 (2007), `hep-ph/0609292`.
[11] S. King, P. White, Phys.Rev. **D52**, 4183 (1995).
[12] S. King, M. Mühlleitner, R. Nevzorov, Nucl.Phys. **B860**, 207 (2012).
[13] J. Baglio, T. Dao, R. Gröber, M. Mühlleitner, H. Rzehak, M. Spira, J. Streicher, K. Walz, *in preparation*.